YAMAMOTO, A. (1982*a*). Unpublished.
YAMAMOTO, A. (1982*b*). *Acta Cryst.* A**38**, 87–92.
YAMAMOTO, A., JANSSEN, T., JANNER, A. & DE WOOLFF, P. M. (1985). *Acta Cryst.* A**41**, 418–530.
YAMAMOTO, A., ONODA, M., TAKAYAMA-MUROMACHI, E., IZUMI, F., ISHIGAKI, T. & ASANO, H. (1990). *Phys. Rev. B*, **42**, 4228–4239.
YAN, Y. F., LI, C. Z., CHU, X., WANG, J. H., FUNG, K. K., CHANG, Y. C., CHEN, G. H., ZHENG, D. N., MAI, Z. H., YANG, Q. S. & ZHAO, Z. X. (1988). *Mod. Phys. Lett.* B**2**, 571–575.
ZANDBERGEN, H. W., GROEN, W. A., MIJLHOFF, F. C., VAN TENDELOO, G. & AMELINCKX, S. (1988). *Physica*, C**156**, 325–354.

Acta Cryst. (1992). B**48**, 134–144

$La_{1.16}Mo_8O_{16}$: a Hollandite-Related Compound with an Incommensurate Modulated Structure

BY H. LELIGNY, PH. LABBÉ, M. LEDÉSERT AND B. RAVEAU

Laboratoire CRISMAT, ISMRa, Bd du Maréchal Juin, 14050 *Caen CEDEX, France*

AND C. VALDEZ AND W. H. MCCARROLL

Chemistry Department, Rider College, POB 6400, *Lawrenceville, NJ* 08648, *USA*

(*Received* 24 *April* 1991; *accepted* 1 *November* 1991)

Abstract

The hollandite-related structure $La_{1.16}Mo_8O_{16}$, M_r = 1184.66, tetragonal, $P4/1$, $a = 9.983$ (1), c = 2.8890 (5) Å, $V = 287.9$ Å^3, $Z = 1$, $D_x = 6.83$ g cm^{-3}, λ(Mo $K\alpha$) = 0.71069 Å, $\mu = 126$ cm^{-1}, $F(0000)$ = 530, room temperature, $R = 0.041$ for 1145 unique reflections with $I \geq 3\sigma(I)$. At room temperature the compound exhibits a one-dimensional incommensurate modulated structure with a modulation wavevector $\mathbf{q}^* = 0.608\,(1)\mathbf{c}^*$. Both a displacive modulation wave, acting on La, Mo and O atoms, and a modulation wave governing the occupancy probability of La sites inside the tunnels are involved in the crystal. Within the superspace group $P4/1$, the final R values of main reflections (477) and first- and second-order satellite reflections (523 and 145) are 0.030, 0.050 and 0.133 respectively. The more spectacular modulation features are the occurrence of La—La pairs in the tunnels and the formation of Mo_3 triangular clusters in the double chains of edge-sharing octahedra. Contrary to previous descriptions based upon rigid tunnels in structures of the hollandite type, the tunnels in the crystal studied are distorted in a periodic way along [001] (λ = 4.75 Å), giving rise to alternate contractions and expansions. The distortion of the double octahedral chains is considerable and probably created *via* the La—O(1) bonds by insertion of La atoms inside two adjacent tunnels.

Introduction

Oxides with the hollandite structure, corresponding to the general formula $A_xM_8O_{16}$ (A = Ba, Pb, K, Rb, Tl, Na; M = Ti, Mn, Fe, Mg, Mo...) form a large family and have been extensively studied for both their ionic conductivity and as encapsulants for radioactive waste. The structural principle of these materials is well established since many structure determinations of synthetic and mineral hollandites have been performed by means of X-ray and neutron diffraction; see, for instance, Sinclair, McLaughlin & Ringwood (1980), Torardi & McCarley (1981), Post, Von Dreele & Buseck (1982), Sinclair & McLaughlin (1982), Torardi & Calabrese (1984), Vicat, Fanchon, Strobel & Tran Qui (1986), Cheary & Squadrito (1989) and Cheary (1990). These oxides have also been studied by electron diffraction and high-resolution microscopy (Bursill & Grzinic, 1980; Mijlhoff, Ijdo & Zandbergen, 1985; Xiang, Fan, Wu, Li & Pan, 1990).

At first sight the $[M_8O_{16}]_\infty$ host lattice is very simple. It consists of infinite rutile chains sharing the edges and the corners of their MO_6 octahedra and forming large square tunnels where the A cations are located. In general, however, the actual structure of these compounds is more complex than can be described by these basic structural principles. A great number of these oxides exhibit superstructures, which have not yet been completely elucidated. This is the case for instance for the non-stoichiometric hollandites $Ba_xTi_{8-x}Mg_xO_{16}$ and $Ba_xTi_{8-2x}Ga_{2x}O_{16}$ with $0.8 < x < 1.33$ (Bursill & Grzinic, 1980), which exhibit a continuous variation of superlattice periodicity and multiplicity. Very complex phenomena can occur as shown by the recent electron diffraction study of the mineral ankangite $Ba_{0.8}(Ti,V,Cr)_8O_{16}$ by Xiang *et al.* (1990). These authors have shown that

0108-7681/92/020134-11$03.00

this mineral exhibits an incommensurate modulated structure.

Molybdenum oxides, which exhibit a tunnel-like structure closely related to the mineral hollandite are of great interest owing to the particular behaviour of molybdenum, which in these oxides is characterized by the unusual mixed valency Mo^{III}/Mo^{IV}. This is also the case for the oxides $K_2Mo_8O_{16}$ (Torardi & Calabrese, 1984) and $Ba_{1.13}Mo_8O_{16}$ (Torardi & McCarley, 1981) in which abnormally short Mo—Mo bonds are observed, and which leads to the formation of Mo_4 metallic clusters.

This paper describes the synthesis and structure of the hollandite-type oxide $La_{1.16}Mo_8O_{16}$. The incommensurate character of the superlattice reflections is demonstrated and the modulated structure is determined by single-crystal X-ray diffraction study.

Experimental

Crystal synthesis

The synthesis method used parallels that described previously for the single-crystal preparation of a variety of reduced oxides of molybdenum with the rare earths (McCarroll, Darling & Jakubicki, 1983). The crystals were prepared by electrolysis of a melt made from a mixture with the molar composition Na_2MoO_4:MoO_3:La_2O_3 = 3.50:3.30:1.00. The electrolysis was carried out in a high-density alumina crucible (McDanel 997) at 1343 K for 45 min using Pt-foil electrodes and with a current of 60 mA after allowing the melt to equilibrate for several hours. The product grows out from the cathode in the form of square prisms and twinned hollow tubes which are often contaminated with other reduced phases and the matrix from which the reduced phases could be separated by alternate washings in hot, dilute HCl and K_2CO_3 solutions. A combination of mechanical separation and dilute nitric acid washes were reasonably effective in isolating the hollandite-type crystals.

X-ray diffraction diagrams: the unusual behaviour of superstructure reflections

The X-ray diffraction photographs, recorded at room temperature, show both main reflections corresponding to the classical cell a = 10.0, c = 2.9 Å, and additional reflections which on cursory examination are indicative of a superstructure of fifth order along the **c** axis. Indeed, oscillating crystal diagrams ([001] rotation axis) show strong main reflections on 0,5,10... levels and superstructure reflections which are missing or very weak on the first and fourth levels, weak on the second and reinforced on the third level. On Weissenberg and precession photographs it is observed that one reflection out of two is systematically missing; the reflection condition $h + k + l = 2n$ for the main spots (h, k, l indexes are related to the subcell) is indicative of an I sublattice. The reflection conditions occurring for the additional spots, $h' + k' = 2n + 1$ for $l' = 10n \pm 1$ and $l' = 10n \pm 2$, $h' + k' = 2n$ for $l' = 10n \pm 3$ and $l' = 10n \pm 4$ (h', k', l' indexes are related to the supercell) cannot easily be explained within a standard space group. The difficulty is overcome if the superstructure reflections are considered as first-order and second-order satellite reflections defined by the modulation wavevector $\mathbf{q}^* = \frac{3}{5}\mathbf{c}^*$ (Fig. 1). Then, the whole reflections are described by four integers h, k, l, m, using the diffraction vector $\mathbf{s}^* = h\mathbf{a}^* + k\mathbf{b}^* + l\mathbf{c}^* + m\mathbf{q}^*$ where m is the satellite order. Within this description only one reflection condition is found: $h + k + l = 2n$ for h, k, l, m, meaning that satellites are located along **c** on both sides of the main reflections.

Symmetry tests: departure from the commensurability

To confirm that the Laue symmetry was $4/m$ and not the lower symmetry $2/m$ and also to verify the previous extinction rule, 2319 h', k', l' reflections, belonging to four octants, were collected with an Enraf–Nonius CAD-4 diffractometer. The intensities $I_{h'k'l'}$ of equivalent reflections were corrected for Lorentz and polarization effects and then compared to their mean value $\langle I \rangle$ through

$$R_{\text{int}} = \sum_{h'k'l'} |\langle I \rangle - I_{h'k'l'}| / \sum_{h'k'l'} I_{h'k'l'}.$$

Before correction for absorption, R_{int} was equal to 0.085 and after correction it reduced to 0.022,

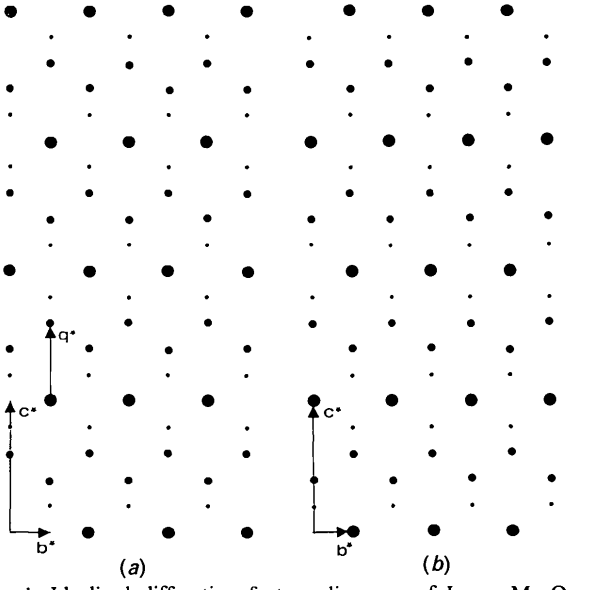

Fig. 1. Idealized diffraction feature diagrams of $La_{1.2-\varepsilon}Mo_8O_{16}$ (ε=0.04). Main reflections and first- and second-order satellite reflections are symbolized by large, medium and small circles respectively. (*a*) Reciprocal levels for $h = 2n$. (*b*) Reciprocal levels for $h = 2n + 1$.

excluding within experimental error the $2/m$ Laue symmetry. In agreement with this result, no significant difference was observed between the a and b parameters, and the γ angle was found equal to $\pi/2$. Moreover, the previous extinction rule was confirmed.

To specify the q_3^* component of $\mathbf{q}^*$ the following process was used: firstly, the a, b, c subcell parameters were refined by least squares from the θ measurement of 21 main reflections; secondly, within the supercell basis, the θ_s angles of ten first-order satellites and their equivalents, corresponding to the smallest integers h' and k', were carefully measured; the averaged values $\langle\theta_s\rangle$ were compared with the calculated ones within the supercell assumption that $c' = 5c$. Significant and systematic discrepancies between these values were then observed allowing a least-squares refinement of q_3^* to be achieved, leading to $q_3^* = 0.608\,(1)$. This departure from the value of 3/5 results from the incommensurate modulated structure.

The main reflections, and the first- and second-order satellite reflections (the third order was not observed) were collected at room temperature with an Enraf–Nonius CAD-4 diffractometer.

The intensities of 1145 unique reflections h, k, l, m with $I \geq 3\sigma(I)$ were corrected for Lorentz, polarization and absorption effects and used to refine the modulated structure. The main features of the data collection are summarized in Table 1.†

Table 1. *Experimental data for* $La_{1.2-\varepsilon}Mo_8O_{16}$

Crystal size	26 × 90 × 208 μm
Lattice parameters (T = 294 K)	a = 9.983 (1), c = 2.8890 (5) Å
Modulation wavevector	$\mathbf{q}^*$[0, 0, 0.608 (1)]
Modulation period	$\lambda = 1/q^* = 4.752$ Å
Superspace group	P_1^{I4}
D_x	6.83 g cm^{-3}
Z	1
M_r	1184.66
V	287.9 Å^3
$F(0000)$	530
Data-collection technique	Enraf–Nonius CAD-4 diffractometer
Scan mode	ω, $4/3\theta$
Wavelength	λ(Mo $K\alpha$) = 0.71069 Å
$(\sin\theta/\lambda)_{max}$	0.995 Å^{-1}
Registered space	$h \geq 0$, $k \geq 0$, $l \geq 0$ $h_{max} = k_{max} = 19$, $l_{max} = 3$, $m_{max} = 2$
Control of intensities	Three reflections every 3000 s; no significant fluctuation observed
No. of reflections measured	2424
No. of reflections with $I \geq 3\sigma(I)$	$hkl0$ 477 $hkl \pm 1$ 523 $hkl \pm 2$ 145
Absorption correction	Based on the crystal morphology
Absorption coefficient	μ(Mo $K\alpha$) = 126 cm^{-1}
Transmission-factor range	0.490–0.818
No. of divisions used in integral calculation of structure factors by the Gaussian method	12
Atomic scattering factors and f', f'' values	*International Tables for X-ray Crystallography* (1974, Vol. IV)

The average structure

The extinction rule concerning the main reflections is consistent with the three space groups $I4/m$, $I\bar{4}$ and $I4$. The average structure was determined assuming the $I4/m$ space group, the refinements were carried out with internal *SDP* programs (B. A. Frenz & Associates Inc., 1982) using the main reflections; the starting values for the atomic positions were taken from the priderite structure (Post *et al.*, 1982). In the initial refinement the lanthanum atom was located at the 0,0,0 site. Subsequent Fourier difference synthesis showed significant residual peaks spread along the **c** axis on both sides of the origin; such features were not observed around the average positions of the molybdenum and oxygen atoms. Consequently, in the final stages of refinement, only the La site was split into two pseudosites 0,0,z and 0,0,$-z$ in order to take account of the spread of electronic density around the average position. β_{ij} thermal parameters were introduced for all atoms. The reliability factors were $R = 0.053$ and $wR = 0.058$ for the 477 main reflections used.

These refinements yield the two following significant results: (i) The two La pseudosites are 0.6 Å from each other along the **c** axis. (ii) The mean occupancy of each La pseudosite is slightly lower than 0.6/2 leading to the approximate chemical formula $La_{1.2-\varepsilon}Mo_8O_{16}$ where $\varepsilon = 0.04$ in our crystal on the basis of the experimental occupancy factor for La.

The first result is in agreement with a displacive modulation occuring mainly for the La atoms. The second result suggests that the occupancy of the La sites is modulated in the actual crystal. Consequently, one can imagine an ideal crystal ($\mathbf{q}^* = \frac{3}{5}\mathbf{c}^*$) where the La atoms would occupy three sites out of five, so leading to empty La sites (e), isolated La atoms (i), and lanthanum pairs (p) ordered along the **c** axis according to the sequence i, e, p, e, i, e, p, e, i... . The lanthanum pairs would result from a displacive modulation. Indeed, two neighbouring La atoms in the basic positions display a very short La—La distance along [001] (c = 2.89 Å) and therefore would want to move in opposite directions, to alleviate the strong repulsive interaction.

A (001) plane projection of the basic structure of this modulated crystal is shown in Fig. 2. This resolution of the average structure within the $I4/m$ space group confirms the classical hollandite $[Mo_8O_{16}]_\infty$ framework. The latter is built up from double edge-sharing rutile chains $[Mo_2O_4]_\infty$. Four $[Mo_2O_4]_\infty$ double chains share the corners of their

† Lists of structure factors have been deposited with the British Library Document Supply Centre as Supplementary Publication No. SUP 54675 (5 pp.). Copies may be obtained through The Technical Editor, International Union of Crystallography, 5 Abbey Square, Chester CH1 2HU, England.

MoO_6 octahedra (Fig. 3), forming large square tunnels running along **c**. It is worth pointing out that in the $[Mo_2O_4]_\infty$ double chains, the O—O edges shared between two adjacent octahedra derived from each other by a 2_1 axis are longer (3.19 Å) than the other edges (2.75 to 2.91 Å). The Mo—Mo bonds along **c** are relaxed (2.899 Å), compared to the diagonal Mo—Mo bonds (2.654 Å). Molybdenum is off-centered in its octahedron leading to two sets of Mo—O bonds (2.02 and 2.08 Å). The lanthanum atoms are located in tunnels, on the axis, where they exhibit a regular square-prismatic coordination, characterized by eight equal La—O distances which are close to 2.59 Å.

This type of infinite double chain of bonded molybdenums derived from rhombohedral metal clusters that share opposite edges was first observed in $NaMo_2O_4$ (McCarley, Lii, Edwards & Brough, 1985) and was later shown by Tarascon (1986) to be part of a more general system which can be formulated $Na_xMo_2O_4$ where $0.55 < x < 1.9$. The structure of this compound is quite different from the hollandite type and consists of layers which have the composition MoO_2 and are separated from each other by the insertion of varying amounts of sodium between the layers.

The average valency of molybdenum in $La_{1.16}Mo_8O_{16}$, calculated from the Mo—O distances of the average structure *via* the equation of Bart & Ragaini (1979) was found to be 3.61, which is in very good agreement with the value of 3.565 which is based upon the above formula. The bonding electron count obtained from the semi-empirical equation $d(n) = 2.614 - 0.6\log n$, where $d(n)$ is the observed distance of a metal–metal bond having order n (McCarley, 1986), yielded a value of 4.80 electrons per Mo_2O_4, corresponding to an average valence of 3.60 for each Mo if all metal electrons are utilized in metal–metal bonding.

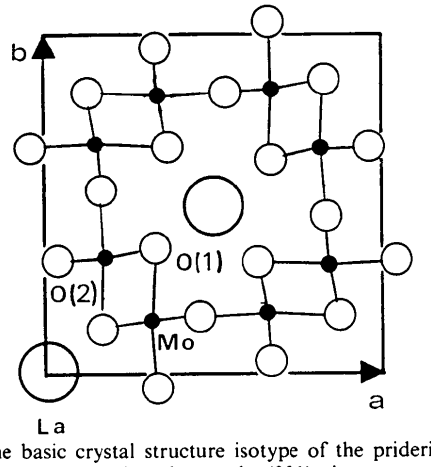

Fig. 2. The basic crystal structure isotype of the priderite structure, projected onto the (001) plane.

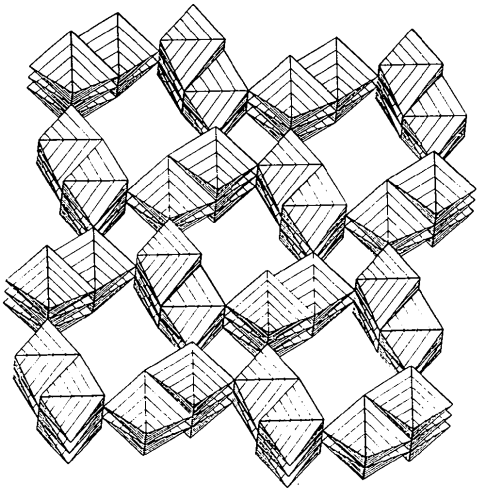

Fig. 3. View of the double octahedral chains and the large [001] tunnels of the basic crystal.

The modulated crystal

Structure determination

Two kinds of modulation wave have to be introduced: a displacive modulation wave which mainly describes the La-atom displacements and a density modulation wave which describes the occupancy probability of the La sites. So, in the unit cell defined by **p**, the displacement of the μth atom from its average position $\mathbf{r}_0^\mu + \mathbf{p}$ is given by $\mathbf{U}^\mu[\mathbf{q}^*.(\mathbf{r}_0^\mu + \mathbf{p})]$ where $\mathbf{q}^*$ is the modulation wavevector and $\mathbf{U}^\mu$ is a periodic vector field of the internal parameter $\bar{x}_4^\mu = \mathbf{q}^*.\mathbf{r}_0^\mu + t$, where t is the phase factor. The occupancy of the La sites is described by the scalar function:

$$P'^\mu(\bar{x}_4^\mu) = P_0^\mu + P^\mu(\bar{x}_4^\mu)$$

where $P_0^\mu = \langle P'^\mu \rangle$. $P^\mu(\bar{x}_4^\mu)$ and the components of $\mathbf{U}^\mu(\bar{x}_4^\mu)$ are expanded in terms of a Fourier series up to second order since the maximum order of observed satellites is two.

$$P^\mu(\bar{x}_4^\mu) = \sum_{n=1}^{2}(C_n^\mu \cos 2\pi n\bar{x}_4^\mu + D_n^\mu \sin 2\pi n\bar{x}_4^\mu).$$

$$U_i^\mu(\bar{x}_4^\mu) = \sum_{n=0}^{2}(A_{i,n}^\mu \cos 2\pi n\bar{x}_4^\mu + B_{i,n}^\mu \sin 2\pi n\bar{x}_4^\mu), \quad i = 1,2,3$$

where n is the harmonic order. The true average position $\mathbf{r}_0^\mu$ of the μth atom is defined by

$$\mathbf{r}_0^\mu = \mathbf{r}_b^\mu + \sum_{i=1}^{3} A_{i,0}^\mu \mathbf{a}_i,$$

where $\{\mathbf{a}_i\}$ are the basis vectors **a**, **b**, **c**, $\mathbf{r}_b^\mu$ is the approximate average position determined from the average structure study and $A_{i,0}^\mu$ are the zero-order Fourier terms. Since the crystal is characterized by a one-dimensionally modulated structure, its symmetry

Table 2. *Effect of the site symmetry requirements on the atomic modulation waves*

The point-group symmetries to be considered are: $4/m$ for La atoms, and m for Mo and O atoms in $P^{I4/m}_{1\ 1}$; $\bar{4}$ and 4 for La atoms in $P^{I\bar{4}}_{(1,\bar{1})}$ and in P^{I4}_{1}. Column 1 is related to the zeroth-order Fourier term, 2 and 3 to the Fourier terms of the first harmonic, 4 and 5 to those of the second harmonic.

Site symmetry		Fourier terms 1	2	3	4	5
$4/m$ and $\bar{4}$	U_1	0	0	0	0	0
	U_2	0	0	0	0	0
	U_3	0	0	$B_{3,1}$	0	$B_{3,2}$
	P'	P_0	C_1	0	C_2	0
m	U_1	$A_{1,0}$	$A_{1,1}$	0	$A_{1,2}$	0
	U_2	$A_{2,0}$	$A_{2,1}$	0	$A_{2,2}$	0
	U_3	0	0	$B_{3,1}$	0	$B_{3,2}$
	P'	P_0	C_1	0	C_2	0
4	U_1	0	0	0	0	0
	U_2	0	0	0	0	0
	U_3	$A_{3,0}$	$A_{3,1}$	$B_{3,1}$	$A_{3,2}$	$B_{3,2}$
	P'	P_0	C_1	D_1	C_2	D_2

is described by introducing a four-dimensional space group (de Wolff, Janssen & Janner, 1981). Three superspace groups, $P^{I4/m}_{1\ 1}$, $P^{I\bar{4}}_{(1,\bar{1})}$ and P^{I4}_{1} are consistent with the unique observed reflection condition: $h + k + l = 2n$ for h, k, l, m.

Restrictions occur on the Fourier terms of P^{μ} and of the $\mathbf{U}^{\mu}$ components if the μth atom is located on a special position in the basic crystal. Denoting the point-group symmetry of the special position by S, the generator operations of S by R, and the associated irreducible translations along the x_4 axis by τ, the restrictions are then found by solving the equations (de Wolff, 1977; de Wolff *et al.*, 1981):

$$\mathbf{U}^{\mu}(\bar{x}^{\mu}_4) = R\mathbf{U}^{\mu}[\varepsilon(\bar{x}^{\mu}_4 - \tau)]$$

and

$$P^{\mu}(\bar{x}^{\mu}_4) = P^{\mu}[\varepsilon(\bar{x}^{\mu}_4 - \tau)].$$

The ε values (± 1) are derived from $R\mathbf{q}^* = \varepsilon\mathbf{q}^*$. For the crystal studied, the τ values associated with the R operations are equal to 0. The Fourier terms required for the atomic modulation waves are shown in Table 2 for the three possible superspace groups.

Refinement of the modulated structure was carried out using the *REMOS* program (Yamamoto, 1982). The quantity minimized was $\chi^2 = (wR)^2 + (\mathrm{pf})^2$ where wR is the weighted R factor and pf is a penalty function which constrains the occupancy probability of an atomic site within reasonable ranges. In a first step the $P^{I4/m}_{1\ 1}$, superspace group was assumed.

An initial modulation model was investigated using only the main reflections and first-order satellites. The refinement was initialized taking into account the splitting of the La sites along **c** in the average structure [this feature gives an approximate value of $|B_{3,1}|$ (Table 2)] and by attributing to C_1 the value $1 - P_o$, with P_o slightly smaller than 0.6. However, as regards molybdenum and oxygen atoms, some trial refinements were necessary in order to arrive at approximate values for the modulation parameters. This modulation model was improved by inclusion of second-order satellite reflections in the refinement. In view of the high reliability factor $R_{h,k,l,\pm 2}$ (R_2) and the systematic discrepancy initially observed between $|F_o|$ and $|F_c|$ ($|F_o| < |F_c|$), a phase fluctuation of the modulation wave (Yamamoto, Nakazawa, Kitamura & Morimoto, 1984) was then considered which led to a significant decrease in R_2. For simplicity, the β_{ij} thermal parameters were assumed to be non-modulated. In order to reduce correlation between these parameters and the Fourier terms describing atomic displacements, alternate refinements were carried out. Satellite reflections were given a greater weight than main reflections.

Table 3. *R reliability factors for the three tested models $P^{I4/m}_{1\ 1}$ (a), $P^{I\bar{4}}_{(1,\bar{1})}$ (b) and P^{I4}_{1} (c)*

R_0, R_1 and R_2 are the reliability factors of the main reflections and first- and second-order satellite reflections respectively. R and wR are the global and weighted global factors. N is the number of parameters, including the scale factor, refined using the *REMOS* program.

	R_0	R_1	R_2	R	wR	N
(*a*)	0.038	0.068	0.153	0.052	0.063	48
(*b*)	0.031	0.053	0.129	0.042	0.050	75
(*c*)	0.030	0.050	0.133	0.041	0.048	78

In a second step, refinements were calculated successively within the two superspace groups $P^{I\bar{4}}_{(1,\bar{1})}$ and P^{I4}_{1}, using all reflections and taking the previous model as the starting model. In the P^{I4}_{1} hypothesis, the z coordinate and the $A_{3,1}$ Fourier term of the La atom (Table 2) were fixed at zero so as to define the coordinate-system origin and the phase origin of the modulation wave respectively. Reliability factors related to previous models are given in Table 3.

Assuming that the statistical tests introduced by Hamilton (1965) are applicable, the following two hypotheses were tested: (i) the superspace group is $P^{I4/m}_{1\ 1}$ rather than P^{I4}_{1}, (ii) the superspace group is $P^{I\bar{4}}_{(1,\bar{1})}$ rather than P^{I4}_{1}. These two hypotheses can be rejected at the 0.5% significance level since the R-factor ratios $R' = 1.31$ and $R'' = 1.04$ are respectively greater than $R_{30,1067,0.005} = 1.025$ and $R_{3,1067,0.005} = 1.006$. Hence, it is estimated that the actual modulated structure is better described within the P^{I4}_{1} superspace group. The results of this model are summarized in Table 4. Note that in the crystal the Mo, O(1) and O(2) atoms are shifted by about 0.1 Å along **c** compared with the La atom. This shift is given by $A_{3,0}c$. As illustrated by the Fourier term values of U_i, the displacive modulation wave is anharmonic.

Table 4. *Refinement results*

A_0, A_1, B_1, A_2, B_2 ($\times 10^4$) are the Fourier terms of the modulation functions $U(\bar{x}_4)$ and $P'(\bar{x}_4)$, β_{ij} ($\times 10^4$) the thermal parameters and B_{44} ($\times 10^4$) the phason terms (e.s.d.'s in parentheses) related to the chosen model (P'_1^4). The molybdenum and oxygen sites are fully occupied within experimental error. x, y, z are the atomic positional parameters derived from the average structure study, assuming space group $I4/m$. Within space group $I4$, the atomic basis positions are $x + A_{0,1}$, $y + A_{0,2}$, $z + A_{0,3}$. $(\Delta/\sigma)_{max} = 0.1$.

				A_0	A_1	B_1	A_2	B_2
La	x	0	U_1	0	0	0	0	0
	y	0	U_2	0	0	0	0	0
	z	0	U_3	0	0	−1576 (14)	−282 (29)	53 (33)
			P'	5800 (50)	5414 (44)	−938 (159)	−841 (52)	358 (96)
Mo	x	3184 (1)	U_1	4 (0)	23 (0)	18 (2)	10 (4)	56 (1)
	y	1619 (1)	U_2	−5 (0)	−90 (0)	−10 (4)	33 (2)	−29 (3)
	z	0	U_3	346 (33)	187 (21)	485 (7)	122 (40)	388 (14)
O(1)	x	3289 (7)	U_1	−7 (3)	−121 (8)	90 (14)	10 (19)	26 (15)
	y	3689 (7)	U_2	−8 (3)	−83 (9)	114 (13)	57 (19)	1 (15)
	z	0	U_3	364 (60)	−72 (81)	18 (39)	−246 (67)	13 (104)
O(2)	x	400 (6)	U_1	−1 (2)	57 (4)	−21 (10)	23 (11)	76 (7)
	y	3316 (6)	U_2	−3 (2)	−38 (4)	−7 (12)	32 (9)	−7 (12)
	z	0	U_3	289 (55)	−130 (53)	26 (25)	−174 (64)	17 (40)

	β_{11}	β_{22}	β_{33}	β_{23}	β_{31}	β_{12}	B_{44}
La	15 (0)	15 (0)	184 (15)	0	0	0	1440 (42)
Mo	8 (0)	9 (0)	16 (5)	9 (2)	−11 (2)	−1 (0)	3313 (46)
O(1)	10 (2)	9 (2)	171 (43)	5 (17)	39 (17)	−3 (1)	3539 (452)
O(2)	3 (1)	17 (1)	154 (37)	−22 (17)	−33 (14)	−2 (1)	149 (383)

Discussion

The occupancy probability variation of the La sites *versus* the $\bar{x}_4$ internal parameter is shown in Fig. 4. The small departure from the expected range of values can be explained by truncation of the Fourier expansion. For comparison purposes the curve $P'(\bar{x}_4)$ related to the ideal crystal ($P_o = 0.60$, $q_3^* = \frac{3}{5}$) is also included; only points on this curve, corresponding to 0, $\frac{1}{5}$, $\frac{2}{5}$, $\frac{3}{5}$ and $\frac{4}{5}$ $\bar{x}_4$ values should to be considered. One observes that the P' function of the actual crystal deviates significantly from the Fourier series expansion, up to second order, of the P' crenellated function associated with the ideal crystal. Moreover, these results confirm that the actual crystal exhibits, like the ideal one, vacant La sites.

The most remarkable features of the modulated structure are the occurence of lanthanum pairs inside the [001] tunnels and correlatively the occurrence of Mo_3 triangular clusters within the double chains of edge-sharing O_6 octahedra.

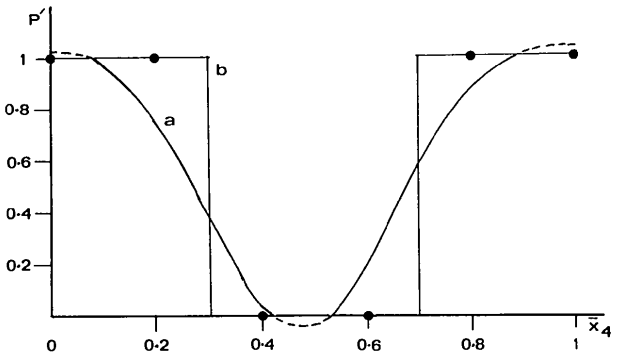

Fig. 4. The occupancy probability P' of the La sites *versus* the $\bar{x}_4$ internal parameter. Inside the actual crystal (curve *a*). Inside the ideal crystal (curve *b*; see text).

The variation of the distance d between two neighbouring La atoms, *versus* the phase factor t, is shown in Fig. 5; the corresponding curve is related to the origin tunnels, *i.e.* centred at the origin of the unit cells. In the unit cell $\mathbf{p}$ ($\mathbf{p} = n_1\mathbf{a} + n_2\mathbf{b} + n_3\mathbf{c}$, n_1, n_2, n_3 integers), the distance $d(t)$ is then obtained which gives a t value of $q_3^* n_3$. As regards the equivalent tunnels (I lattice), the La—La distances to be considered are $d(t - q_3^*/2)$. The unbroken part of the curve (Fig. 5) is related to the lanthanum pairs, the shortest La—La distance being assumed to be about 3.50 Å; such a distance is found in the compound La_7Ni_3 for instance (Fischer, Hälg, Schlapbach & Yvon, 1978). Moreover, this minimal-distance value for an La—La pair is supported by the fact that the approximate probability of smaller distances, as deduced from our calculations, is less than 0.45 and rapidly tends towards zero as the La—La distance decreases. The largest La—La distance observed in the crystal studied was 3.75 (1) Å. Since the occupancy probabilities of two neighbouring La sites are given by $P'(\bar{x}_4)$ and $P'(\bar{x}_4 + q_3)$, consideration of the curve shape $P'(\bar{x}_4)$ (Fig. 4), related to the actual crystal, allows one to conclude that lanthanum pairs with distances ranging from 3.72 to 3.75 Å occur with the largest probabilities; moreover, the value of this probability for such distances remains approximately constant *versus* t and is close to 2/3.

The occurrence of ion pairs inside a crystal has already been observed; for example in the compound $Ba_5(Mo_4O_6)_8$ (Torardi & McCarley, 1986; McCarley, 1986). Within the superlattice, five Ba^{2+} sites out of eight are occupied in an ordered way, giving

rise to barium pairs chacterized by a distance of 3.66 Å.

In the crystal studied isolated La atoms were also found, as is the case in the ideal crystal, with site occupancy probabilities ranging from 0.92 to 1. La sites close to the La_2 pair sites exhibit an occupancy probability smaller than 0.5, in agreement with the fact that the presence of an La_2 pair rules out the existence of a lanthanum cation in an adjacent site. As a result of the incommensurate character of the modulation, the likely lanthanum pairs are not distributed through the [001] tunnels in the same way as in the ideal crystal. Considering for instance the origin tunnels and defining the positions of the lanthanum pairs along [001] by the n_3 integers, the nominal sequence of these pairs is 2, 7, 10, 15, 20, 25, 30, 35, 38, 43, 48..., while in the ideal crystal the sequence is regular with the succession 2, 7, 12, 17, 22.... Consequently, in the actual crystal, locally there may be groups of two neighbouring pairs much closer than other pairs.

The variations of vertical Mo—Mo distances (parallel to the tunnels) and of diagonal Mo—Mo distances, *versus* the t phase factor, are illustrated in Figs. 6(*a*) and 6(*b*) respectively. Two curves are drawn on each figure and the circled numbers specify the two types of Mo—Mo distances considered as defined in Fig. 6(*c*). These distances exhibit large variations throughout the crystal: 2.47 to 3.16 Å for the vertical bonds, 2.47 to 3.03 Å for the diagonal bonds. The standard deviations are about 0.015 Å.

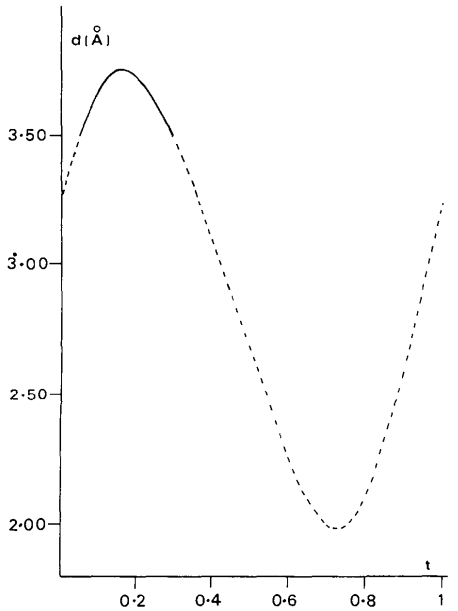

Fig. 5. La—La pairs inside the [001] tunnels of the crystal. The unbroken part of the curve describes (*versus* the phase factor t) the variation of La—La distance relative to the pairs occurring in the origin tunnels (see text).

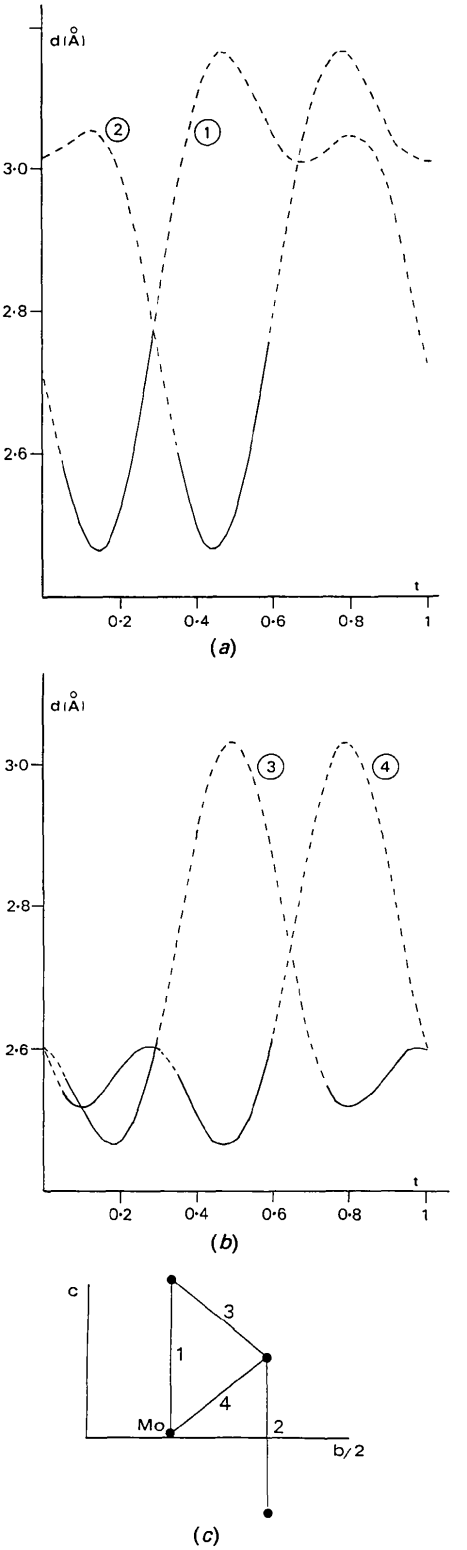

Fig. 6. Variation of the Mo—Mo distance in the double octahedral chains *versus* the phase factor t. (*a*) Bonds parallel to the tunnels. (*b*) Diagonal bonds. (*c*) Arrangement of the Mo atoms considered in the basic crystal; projection onto the (100) plane.

The unbroken parts of the curves are related to the observed distances within the unit cells where the lanthanum pairs occur. These distances, ranging from 2.47 to 2.60 Å for the diagonal Mo—Mo bonds and from 2.47 to 2.76 Å for the vertical Mo—Mo bonds, are typical of those found in a variety of Mo oxides containing metal–metal bonds. From the previous features it is concluded that Mo_3 triangular clusters are formed within the double octahedral chains and these clusters occur in the neighbourhood of the lanthanum pairs. This remarkable property is illustrated in Fig. 7, which shows the modulated structure in the first five unit cells of the crystal.

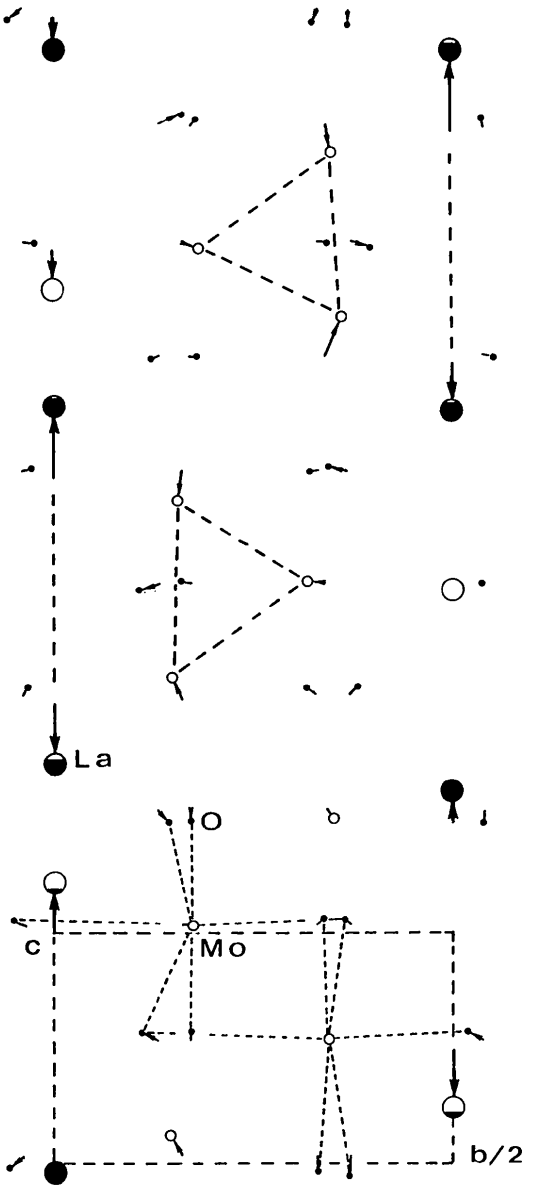

Fig. 7. [100] projection of the modulated structure through the first five unit cells. Atomic displacements from the average positions are exaggerated for clarity and the largest are marked with arrows. The solid part of the large circles represents the La sites occupancy probability; the La—La pairs and Mo_3 triangular clusters are shown with dashed lines. Mo—O bonds occurring in the O_6 octahedra are represented, inside the origin unit cell, by dotted lines.

Regular or very nearly regular Mo_3 clusters are well established in molybdenum oxide systems when the average valence of molybdenum is between 3.33 and 4 (McCarroll, Katz & Ward, 1957; Torardi & McCarley, 1985; Betteridge, Cheetham, Howard, Jakubicki & McCarroll, 1984; Aleandri & McCarley, 1988).

The Mo—O bond lengths in the O_6 octahedra exhibit variations as large as 15% throughout the crystal (Fig. 8). Such variations of Mo—O distances are also observed in the modulated structure of Mo_8O_{23} (Komdeur, de Boer & van Smaalen, 1990). Correspondingly, the lengths of the edges of the MoO_6 octahedra show considerable variation (Table 5), mainly those of the shared edges (again about 15%). Consequently, atomic displacements observed inside the O_6 octahedra in the crystal studied cannot be interpreted in a satisfactory way with a rigid-body model, even to a rough approximation. This conclusion was reached from a least-squares refinement of the translation and rotation groups and from calculation of an agreement factor with the model being tested. A second model, assuming a distortion described by a symmetrical matrix for the O_6 octahedra, was considered and tested using a least-squares refinement program. The agreement factor for this model was also poor. However, although no simple model is available, an attempt to explain the displacive modulation occuring in the octahedral chains is given in *Concluding remarks*.

The variation of the two sets of La—O bond lengths, *versus* the t phase factor, is shown in Fig. 9. The unbroken parts of the curves are related to bonds established between the oxygen atoms of type O(1) (Fig. 10) and the La atoms of one pair. Examination of Fig. 9 allows the following features to be deduced:

(i) An oxygen atom linked to two La atoms of one pair forms two bonds with similar La—O distances (a and b parts of the two curves); the b part corresponds to the larger distance on curve 2.

(ii) An oxygen atom linked to only one La atom of one pair forms stronger bonds than one linked to two La (c and d parts of the two curves); the d part corresponds to the shorter La—O distance on curve 1, which ranges from 2.38 (2) to 2.51 (2) Å.

(iii) The longer La—O distances of curve 1 and the shorter La—O distances of curve 2, which occur for t values near 0.4, do not contribute significantly to the bonding in the crystal since the occupancy probability of the corresponding La sites is very small or zero.

(iv) For the oxygen atom linked to an isolated La atom, one observes intermediate La—O distances which correspond to t values close to zero and one.

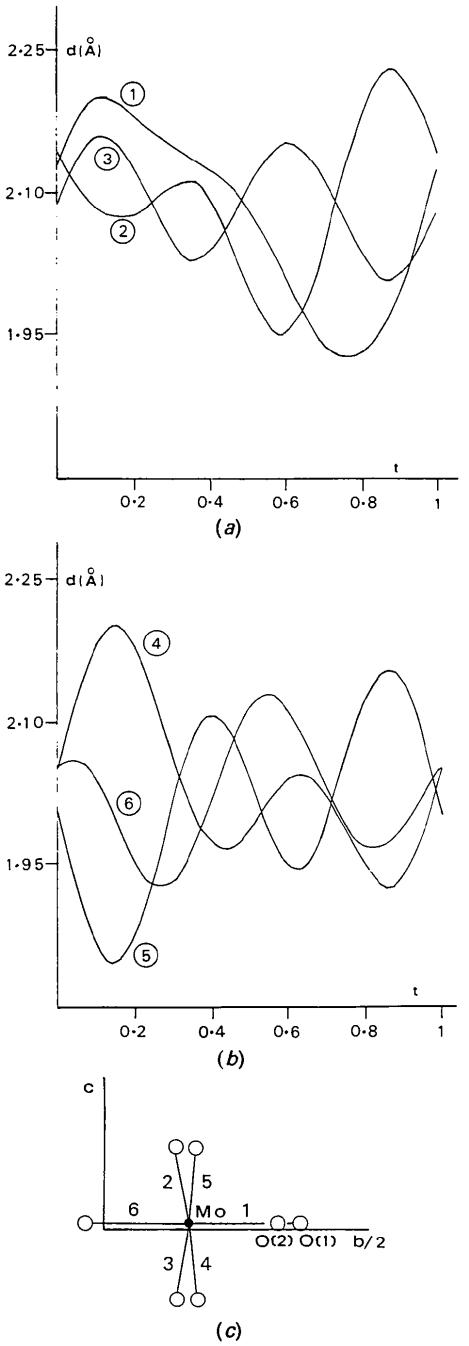

Fig. 8. Mo—O bond-length variation inside the O_6 octahedra *versus* the phase factor t. (*a*) The Mo—O distances specified by the numbers 1, 2 and 3 are distributed around a mean value of about 2.02 (2) Å. (*b*) The Mo—O distances specified by the numbers 4, 5 and 6 are distributed around a mean value of about 2.09 (2) Å. (*c*) A projection of the MoO_6 octahedron in the basic crystal onto the (100) plane.

Table 5. O—O *interatomic distances* (Å) *in the* O_6 *octahedra* (*e.s.d.'s in parentheses*)

$\langle d \rangle = \int_0^1 d(t)\mathrm{d}t$, with t the phase factor.

	$\langle d \rangle$	d_{min}	d_{max}
O(1)—O(2)^{i}	2.78 (3)	2.57 (3)	2.95 (3)
O(1)—O(2)^{ii}	2.81 (3)	2.75 (3)	2.87 (3)
O(1)—O(1)^{i}	3.18 (4)	2.90 (4)	3.37 (4)
O(2)^{iii}—O(2)^{i}	2.84 (2)	2.71 (3)	3.04 (3)
O(2)^{iii}—O(2)^{ii}	2.84 (2)	2.73 (3)	2.96 (2)
O(2)^{iii}—O(1)^{i}	2.76 (3)	2.65 (3)	2.89 (3)
O(2)^{iii}—O(1)^{ii}	2.75 (3)	2.69 (3)	2.79 (3)
O(2)^{i}—O(1)^{i}	2.90 (3)	2.71 (3)	3.17 (3)
O(2)^{i}—O(2)^{ii}	2.89 (4)	2.77 (3)	3.00 (4)
O(1)^{i}—O(1)^{ii}	2.90 (5)	2.80 (5)	3.02 (5)

Symmetry code: (i) $\frac{1}{2}-x', \frac{1}{2}-y', \frac{1}{2}+z'$; (ii) $\frac{1}{2}-x', \frac{1}{2}-y', -\frac{1}{2}+z'$; (iii) $y', -x', z'$. x', y', z' are the average atomic coordinates within space group $I4$.

(v) As a result of modulation features, each La atom of one pair exhibits a very distorted square prismatic coordination while isolated La atoms exhibit rather regular square-prismatic coordination.

While the incommensurate behaviour observed here would seem to arise primarily as a result of attempting to provide the most stable environment possible for lanthanum which cannot be achieved in the average structure, the possible influence of small amounts of impurities cannot be overlooked. There seems to be little question that some aluminum is extracted from the crucible during electrolysis and it is observed that the growth of hollandite-type crystals occurs only after the crucible has been soaked for several hours in the melt or if some silica is added, in which case the formation of a monoclinic form of the compound predominates. Often, the

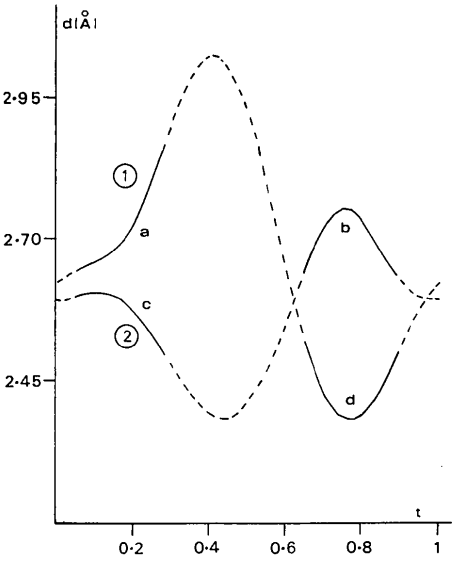

Fig. 9. Variation *versus* the phase factor t, of the two La—O independent bond lengths.

soaking time can be eliminated or substantially reduced if a crucible which has been used previously is employed. Indeed some semiquantitative analyses for Si and Al indicate that up to 1–2 mol% of these elements might be present. However, the results were complicated by the fact that all samples analysed consisted of a mixture of both forms and it was not clear if these elements were actually incorporated into the crystals or came from the presence of small amounts of $La_3Mo_4SiO_{14}$ or $La_3Mo_4Al_{2/3}Mo_{1/3}O_{14}$, which we know form under the conditions described above and are morphologically similar (but not identical) to the hollandite phase. The fact that we have been unable to prepare the hollandite phase either by reaction of stoichiometric amounts of Mo, MoO_3 and La_2O_3 according to the formula $La_{1+x}Mo_8O_{16}$ ($x = 0.1$–0.3) or by doping similar samples with 1–2 mol% of SiO_2 or Al_2O_3 would tend to support the postulate that these elements in the melt tend to promote growth of the hollandite phase and repress the formation of other phases that form under otherwise similar conditions, such as $LaMo_{7.70}O_{14}$ (Leligny, Ledésert, Labbé, Raveau & McCarroll, 1990).

Concluding remarks

The atomic displacements observed inside the double octahedral chains can be better understood by considering the effect of the La atoms as predominant; indeed, each double octahedral chain is located between two adjacent tunnels (Fig. 3) where the La atoms are distributed in a different manner along [001]. As expected, the O(1) oxygen atoms which are bonded to both La and Mo atoms, experience larger lateral displacements from their basic positions than the O(2) oxygens which are only bonded to Mo [this result is demonstrated by the O(1) and O(2) Fourier terms in Table 4]. As a result, the cross-sectional shape of the tunnels varies drastically along [001]. This is illustrated in Fig. 11 where three configurations, dealing with extreme and mean situations, are drawn for the two adjacent tunnels. The star-like configuration of the tunnel section occurs mainly in the level of the La_2 pairs, *i.e.* when the O(1) atom is bonded to two lanthanum atoms simultaneously. As regards the other configurations no simple explanation is found. These results show, contrary to previous descriptions which consider the hollandite tunnels to be rigid, that in our crystal a periodic distortion of the latter occurs along [001] resulting in alternate shrinkages and expansions. This effect can be explained by the electrostatic attraction of the oxygen O(1) atoms by the highly charged $[La_2]^{6+}$ pairs. Thus, distortion of the MoO_6 octahedra appears to be a consequence of this remarkable phenomenon. A closely related behaviour, involving strong Ba/framework interaction has been observed in the $Ba_{1.2}Ti_{6.8}Mg_{1.2}O_{16}$ hollandite (Fanchon, Vicat, Hodeau, Wolfers, Tran Qui & Strobel, 1987) which at room temperature exhibits an almost commensurate structure with a complex distribution of barium cations in the tunnels. In conclusion, it appears that this incommensurability phenomenon is possibly characteristic of hollandite in which the *A* cation has a formal charge greater than +1, so that several of the previous structure determinations do not perhaps correspond to the actual image of the crystal, but rather to an average structure.

The authors are grateful to Dr A. Yamamoto who kindly sent them the *REMOS* computer program and to Mrs J. Chardon for her technical assistance.

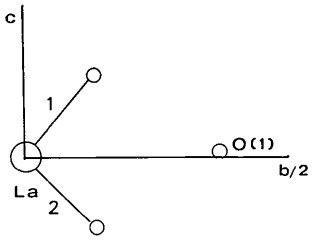

Fig. 10. The two La—O independent bonds in the basic crystal; projection onto the (100) plane.

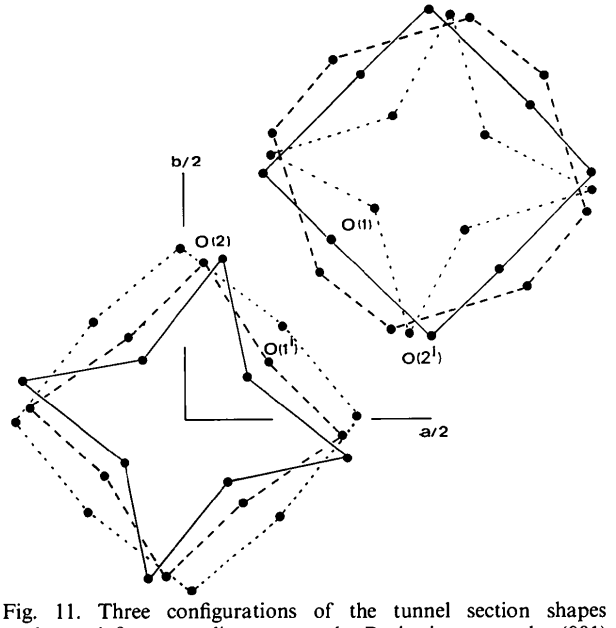

Fig. 11. Three configurations of the tunnel section shapes observed for two adjacent tunnels. Projection onto the (001) plane. The full lines, the dotted lines and the dashed lines are related to t values of 0, 0.40 and 0.80 respectively. The atomic displacements from the basic positions are exaggerated for clarity. The symmetry code used (see Table 5) relates to the basic positions.

References

ALEANDRI, L. E. & MCCARLEY, R. E. (1988). *Inorg. Chem.* **27**, 1041–1044.

B. A. FRENZ & ASSOCIATES INC. (1982). *SDP Structure Determination Package*. College Station, Texas, USA.

BART, J. C. & RAGAINI, V. (1979). *Inorg. Chim. Acta*, **36**, 261–265.

BETTERIDGE, P. W., CHEETHAM, A. K., HOWARD, J. A. K., JAKUBICKI, G. & MCCARROLL, W. H. (1984). *Inorg. Chem.* **23**, 737–740.

BURSILL, L. A. & GRZINIC, G. (1980). *Acta Cryst.* B**36**, 2902–2913.

CHEARY, R. W. (1990). *Acta Cryst.* B**46**, 599–609.

CHEARY, R. W. & SQUADRITO, R. (1989). *Acta Cryst.* B**45**, 205–212.

FANCHON, E., VICAT, J., HODEAU, J.-L., WOLFERS, P., TRAN QUI, D. & STROBEL, P. (1987). *Acta Cryst.* B**43**, 440–448.

FISCHER, P., HÄLG, W., SCHLAPBACH, L. & YVON, K. (1978). *J. Less-Common Met.* **60**, 1–9.

HAMILTON, W. C. (1965). *Acta Cryst.* **18**, 502–510.

KOMDEUR, A. J. H., DE BOER, J. L. & VAN SMAALEN, S. (1990). *J. Phys. Condens. Matter*, **2**, 45–54.

LELIGNY, H., LEDÉSERT, M., LABBÉ, PH., RAVEAU, B. & MCCARROLL, W. H. (1990). *J. Sold State Chem.* **87**, 35–43.

MCCARLEY, R. E. (1986). *Polyhedron*, **5**, 51–61.

MCCARLEY, R. E., LII, K.-H., EDWARDS, P. A. & BROUGH, L. F. (1985). *J. Solid State Chem.* **57**, 17–24.

MCCARROLL, W. H., DARLING, C. & JAKUBICKI, G. (1983). *J. Solid State Chem.* **48**, 189–195.

MCCARROLL, W. H., KATZ, L. & WARD R. (1957). *J. Am. Chem. Soc.* **79**, 5410–5414.

MIJLHOFF, F. C., IJDO, D. J. W. & ZANDBERGEN, H. W. (1985). *Acta Cryst.* B**41**, 98–101.

POST, J. E., VON DREELE, R. B. & BUSECK, P. R. (1982). *Acta Cryst.* B**38**, 1056–1065.

SINCLAIR, W. & MCLAUGHLIN, G. M. (1982). *Acta Cryst.* B**38**, 245–246.

SINCLAIR, W., MCLAUGHLIN, G. M. & RINGWOOD, A. E. (1980). *Acta Cryst.* B**36**, 2913–2918.

TARASCON, J. (1986). *Solid State Ionics*, **22**, 85–96.

TORARDI, C. C. & CALABRESE, J. C. (1984). *Inorg. Chem.* **23**, 3281–3284.

TORARDI, C. C. & MCCARLEY, R. E. (1981). *J. Solid State Chem.* **37**, 393–397.

TORARDI, C. C. & MCCARLEY, R. E. (1985). *Inorg. Chem.* **24**, 476–481.

TORARDI, C. C. & MCCARLEY, R. E. (1986). *J. Less-Common Met.* **116**, 169–186.

VICAT, J., FANCHON, E., STROBEL, P. & TRAN QUI, D. (1986). *Acta Cryst.* B**42**, 162–167.

WOLFF, P. M. DE (1977). *Acta Cryst.* A**33**, 493–497.

WOLFF, P. M. DE, JANSSEN, T. & JANNER, A. (1981). *Acta Cryst.* A**37**, 625–636.

XIANG, S.-B., FAN, H.-F., WU, X.-J., LI, F.-H. & PAN, Q. (1990). *Acta Cryst.* A**46**, 929–934.

YAMAMOTO, A. (1982). *REMOS*. A computer program for the refinement of modulated structures. National Institute for Research in Inorganic materials, Niiharigun, Ibaraki, Japan.

YAMAMOTO, A., NAKAZAWA, H., KITAMURA, M. & MORIMOTO, N. (1984). *Acta Cryst.* B**40**, 228–237.

Acta Cryst. (1992). B**48**, 144–151

Charge Density Around a Jahn–Teller-Distorted Site: $(ND_4)_2Cu(SO_4)_2.6D_2O$ at 85 K

BY BRIAN N. FIGGIS, LECIA KHOR, EDWARD S. KUCHARSKI AND PHILIP A. REYNOLDS

School of Chemistry, University of Western Australia, Nedlands, WA 6009, *Australia*

(*Received* 6 *August* 1991; *accepted* 5 *November* 1991)

Abstract

Diammonium hexaaquacopper(II) disulfate-d_{20}, $[ND_4]_2[Cu(D_2O)_6](SO_4)_2$, $M_r = 419.7$, monoclinic, $P2_1/a$, $a = 9.399$ (2), $b = 12.673$ (2), $c = 6.071$ (1) Å, $\beta = 107.13$ (1)°, $V = 691.1$ (4) Å^3, $Z = 2$, $D_x = 2.02$ Mg m^{-3}, Mo $K\alpha$ radiation, $\lambda = 0.71069$ Å, $\mu = 2.008$ mm^{-1}, $F(000) = 415.3$, $T = 85$ (2) K, $R(I) = 0.020$, $R(F) = 0.014$ for 7287 reflections. The CuO_6 octahedron has a large Jahn–Teller distortion; Cu—O(8) 2.301 (1), Cu—O(7) 2.010 (1), Cu—O(9) 1.960 (1) Å. It was necessary to use quartic anharmonic thermal parameters at the Cu^{II} site. These modelled potential softening associated with the Jahn–Teller distortions, important even at this temperature. At the ammonium, the sulfate and the hexaaqua-ion sites the charge densities, at this experimental accuracy, can be described by simple valence functions which reflect only local symmetry. Large lower-symmetry densities are not observed; any small such effects are comparable with uncertainties in the treatment of the thermal motion. The valence refinement gave Cu 3*d* populations of $3d_{xy}^{1.58\,(6)}3d_{xz,yz}^{2.12\,(3)}3d_{z^2}^{2.18\,(6)}3d_{x^2-y^2}^{0.82\,(7)}$. This shows the hole expected in $3d_{x^2-y^2}$, modified, taking overlap into account, by a covalent σ acceptance of 0.52 (1) and π back donation of 0.18 (10) e. The rhombic distortion causes $3d_{z^2}/3d_{x^2-y^2}$ mixing corresponding to a $3d_{z^2}$ coefficient of -0.21 (7) in a spin-hole wavefunction. Ionic charges from the model are $Cu(OD_2)_6^{1.7+}$, $ND_4^{0.6+}$ and $SO_4^{1.5-}$. These are more ionic than for the isomorphous Cr^{II} salt, where σ and π charge

0108-7681/92/020144-08$03.00